

# TIMING JITTER CHARACTERIZATION AT THE NSLS SDL

H. Qian<sup>#</sup>, Y. Hidaka, J. B. Murphy, B. Podobedov, S. Seletskiy, Y. Shen, X. Yang, X. J. Wang  
 National Synchrotron Light Source, Brookhaven National Laboratory, Upton, NY 11973, U.S.A  
 C.X. Tang<sup>#</sup>, Department of Engineering Physics, Tsinghua University, Beijing 100084, China.

## Abstract

Two novel timing jitter measurement techniques with a 100 fs resolution are presented in this paper. The first technique based on the Schottky effect, is used to measure the timing jitter between the photoinjector drive laser and the RF system; and it was employed to characterize the environment effects on the timing jitter. The I/Q beam monitor based on a stripline beam position monitor (BPM) is used to characterize the electron beam arrival time jitter.

## INTRODUCTION

Stability and reliability are one of the major challenges in operating photoinjectors. Synchronization between the laser system and the accelerator RF system plays a critical role in photoinjector operation, pump-probe experiments and many other applications. Generally speaking, there are two types of timing jitter: one is the timing jitter between the photoinjector drive laser and the linac RF system, and the other is the jitter of electron beam arrive at the interaction point – arrival time jitter.

The NSLS SDL is a laser linac facility dedicated to the high-brightness electron and photon beam R&D and applications [1]. The NSLS SDL consists of a high-brightness 1.6 cell BNL-type photocathode RF gun, a 300 MeV linac, a four-magnet chicane bunch compressor and a FEL system (fig.1). In order to improve the SDL linac and FEL performance, we developed two novel timing jitter measurement techniques: one is based on the Schottky effect, and other is an I/Q beam monitor based on a stripline beam position monitor (BPM). In the rest of this paper, we discuss those two timing jitter measurement techniques and their applications to characterize the SDL photoinjector and linac timing jitter performance.

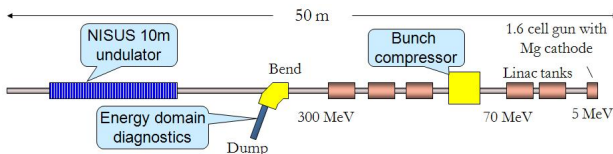


Figure 1: The NSLS SDL schematic layout.

## LASER TIMING JITTER

Two circuits of synchronizing the photoinjector to the RF system are implemented at the SDL (fig.2). One is so called ‘Local mode’, where the laser oscillator cavity is adjusted so it can be synchronized to the 81.6 MHz RF source. And in the other mode, the laser oscillator is used to generate 2856 MHz RF by a 10 GHz fast photodiode.

This is known as the ‘Laser Mode’. In the rest of this section, we will first discuss the timing jitter measurement technique based on the Schottky effect, and then apply this technique to compare the performance of the two modes of the laser synchronization, and study the effect of the laser table temperature fluctuation on the timing jitter.

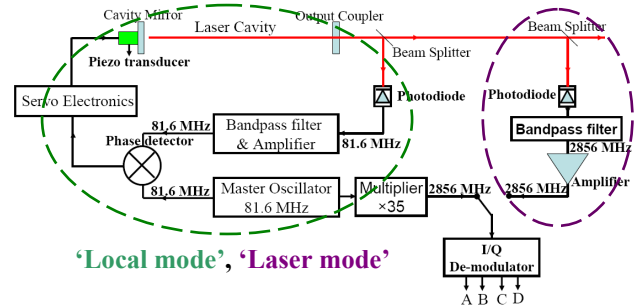


Figure 2: SDL Laser to RF synch circuits.

The total charge emitted from a photocathode can be expressed by the following equation [2 - 4],

$$Q(\phi_g) = A \int d\tau I(\tau) (h\nu - \phi + \alpha\sqrt{\beta E(\phi_g + \tau)})^2 \quad (1)$$

where  $I(\tau)$  is the laser intensity,  $h\nu$  is the photon energy,  $\phi$  is the cathode work function,  $\alpha\sqrt{\beta E(\tau)}$  is the reduced work function by the Schottky effect. For a Cu or an Mg cathode illuminated by a UV laser, the photon energy is close to the cathode’s work function, the photoemission is dominated by the Schottky effect. Furthermore, the total charge escaped from the RF gun is also affected by space charge effect, longitudinal beam dynamics and dark current.

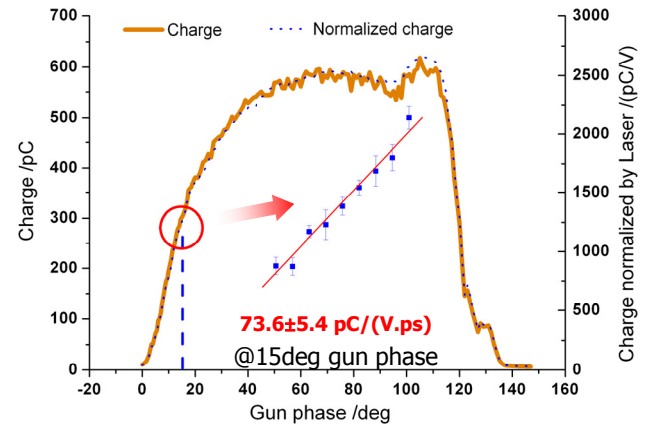


Figure 3: Emitted charge versus RF gun phase (Mg Cathode).

Figure 3 plots the total photoelectron charge versus RF gun phase. This curve contains information on the laser pulse length, RF gun phase and amplitude, so it is very useful in photoinjector operations and diagnostics [4].

<sup>#</sup>hqian@bnl.gov

One of its applications is to characterize the laser to the RF system timing jitter. Taking advantage of the strong dependency of the charge on the RF gun phase either on the rising or falling edges in Fig.3, we could get the timing jitter information of the laser relative to the RF system.

Equation 1 shows that charge fluctuation not only comes from laser to RF timing jitter, but also from the fluctuation of the laser intensity and RF field amplitude. The charge fluctuation caused by the laser intensity instability can be removed by normalization. This requires measuring both charge and laser intensity shot-by-shot simultaneously. RF field amplitude and noise were measured to determine the resolution of this technique.

Normalized charge measurement is done by scanning the gun phase around 15 deg, and the timing jitter calibration value is  $73.6 \pm 0.4$  pC/(V.ps), as shown in figure 3. The measured RMS fluctuation of the RF amplitude is about 0.15%, and the noise contributes to about 2% experimental error. The resolution of this technique is  $\sim 100$  fs.

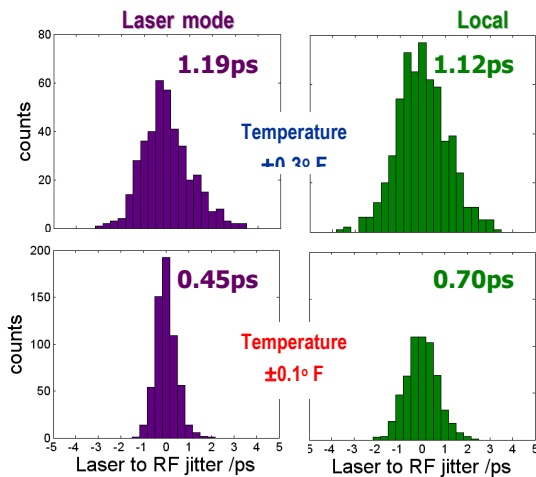


Figure 4: Laser to RF timing jitter characterizations corresponding to the two temperature fluctuations on the laser table.

To characterize the timing jitter between the laser and RF system, the normalized charge was measured over 5 minutes at the RF gun phase of 15 degree. And timing jitter performances of the two synchronization modes (Laser and Local) at the SDL are measured under the different laser room temperature fluctuations, the results are displayed in figure 4. When the p-p temperature fluctuation is  $\pm 0.3^\circ\text{F}$ , the RMS timing jitters of ‘Laser Mode’ and ‘Local Mode’ are 1.19 ps and 1.12 ps, respectively. After the temperature is settled down to the p-p fluctuation of  $\pm 0.1^\circ\text{F}$ , the RMS timing jitters of ‘Laser Mode’ and ‘Local Mode’ are reduced to 0.45 ps and 0.70 ps, respectively. Our measurement indicates ‘Laser mode’ has the advantage over ‘Local mode’ when laser room temperature is stable within  $\pm 0.1^\circ\text{F}$ .

### ARRIVAL TIMING JITTER STUDIES

The source of the arrival time jitter is mainly due to the electron beam energy fluctuation, especially before the electron beam reaches relativistic. The electron beam energy fluctuation could come from either the RF amplitude or the phase. The RF phase fluctuation due to the laser timing jitter was discussed in the previous section. To study the arrival time jitter of the electron beam, a stripline BPM was installed at the exit of the last linac [5].

The BPM is designed to have the SDL linac RF frequency (2856 MHz) as the second-order resonant frequency. This harmonic from the BPM sum signal is first filtered out, and then mixed with the SDL low level RF signal to detect the electron beam phase change, i.e. the electron beam arrival timing change relative to the reference RF system. We introduce a  $90^\circ$  phase shift between the horizontal and vertical plane of the BPM, this will allow us to simultaneously monitoring both the arrival time jitter and electron beam intensity fluctuation (I/Q beam monitor). Furthermore, BPM sum signal used for the intensity monitor is used to normalize the arrival time monitoring signal so the effect of the electron beam charge fluctuation is removed. The schematic of our experiment setup is shown in figure 5.

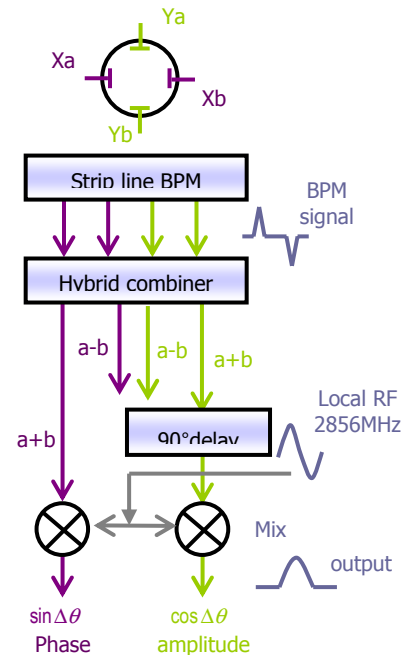


Figure 5: I/Q beam monitor for both arrival time and intensity monitoring.

To understand the effect of the magnetic chicane and linac on the arrival time jitter, PARMELA simulations were performed. In the simulation, a 350 pC electron beam is considered. It is generated by the RF gun at the 30 deg with a peak field of 100MV/m, and then it is accelerated by the first linac, which also removes any residual energy chirp in the electron beam. The second linac operates at the 23 deg before the crest to introduce

an energy chirp for the chicane compression. The average acceleration field for both linac is 11 MV/m. With the chicane on, 1ps of the laser to RF timing jitter leads to 0.38 ps electron beam arrival jitter and 0.22 % relative energy jitter (figure 6). When chicane is off, 1ps of the laser to RF timing jitter will cause 0.69 ps arrival time jitter with much less energy jitter. PARMELA simulation shows that both the RF gun and chicane reduce e<sup>-</sup> beam arrival time jitter when only the timing jitter of the laser system is considered.

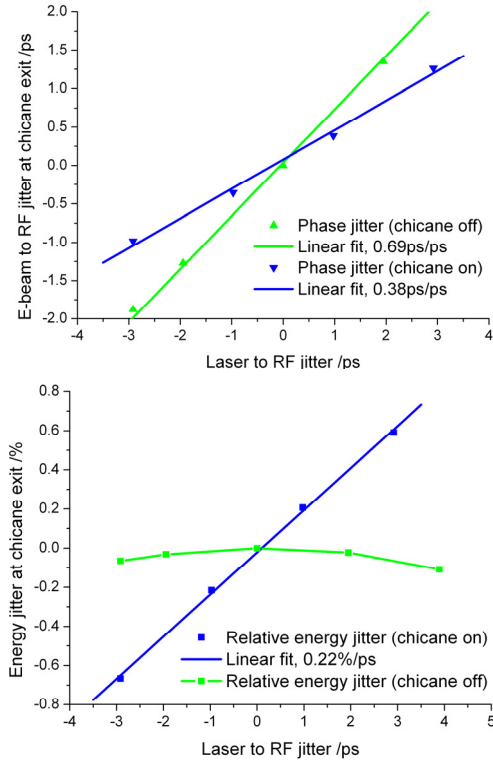


Figure 6: Parmela simulations of e<sup>-</sup> beam arrival jitter (top) and energy jitter (bottom) at the chicane exit.

By varying the phase of the reference RF signal locally, the relationship between normalized mixer output and phase change is calibrated to be  $0.030 \pm 0.01/\text{ps}$  (fig. 7), which means I/Q beam monitor can measure the e-beam arrival time jitter better than 100 fs.

The measurement of electron beam arrival time jitter without the chicane compression is presented here. The RF gun, linac1 and linac2, are all powered by a single klystron, and no energy chirp is introduced in the linac2. Data are recorded in 600 shots for 5 minutes and the RMS arrival jitter is found to be 1.13ps (figure 8), which is much larger than our expectations. Because laser to RF jitter is ~ 0.5 ps, and this jitter is compressed by 30% in the RF gun based on the simulation, the expected RMS e<sup>-</sup> beam arrival time jitter is ~ 0.35 ps. The potential source of this large jitter could be the RF amplitude fluctuation or instability in the RF reference. The disagreement

between simulation and experiment will be investigated in the future.

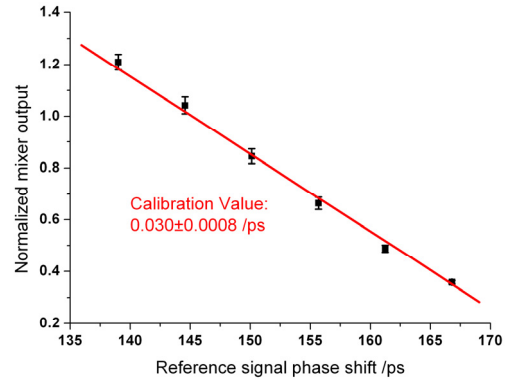


Figure 7: Calibration curve of e-beam arrival jitter

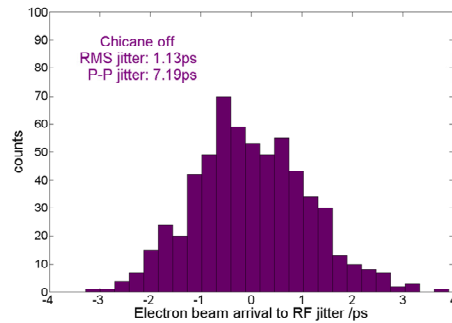


Figure 8: E-beam arrival jitter when chicane is off.

## CONCLUSION

In this paper, we present preliminary experiment studies of two novel timing-jitter measurement techniques. Their effectiveness is demonstrated by characterizing the laser and electron beam to RF timing jitter at the NSLS SDL. The resolutions of both techniques are proved to be ~100 fs.

## ACKNOWLEDGEMENTS

We are grateful for support from the NSLS. This work is supported by the U.S. Department of Energy (DOE) under contract No. DE-AC02-98CH1-886.

## REFERENCES

- [1] J.B. Murphy & X.J. Wang, “Laser-Seeded Free-Electron Lasers at the NSLS”, SRN, 21, 41(2008).
- [2] E.O. Lawrence et al, Phys. Rev., V36, 482, 1930.
- [3] R.H. Fowler, Phys. Rev., 38, 45 (1931).
- [4] X.J. Wang et al, “Challenges of Operating A Photocathode RF Gun”, Proceeding of Linac 98, 866 (1998).
- [5] X.J. Wang et al, “Experimental Characterization of ATF Beam Position Monitors”, Proceeding of 1995 EPAC, 1576 (1995).